J. Fish. Sci. Tech. 1(1), 48~62, 1998

Volume Transport on the Texas-Louisiana Continental Shelf

Kwang-Woo Cho

Research Center for Ocean Industrial Development (RCOID), Pukyong National University, Pusan 608-737, Korea

(Received March 1998, Accepted June 1998)

Seasonal volume transport on the Texas-Louisiana continental shelf is investigated in terms of objectively fitted transport streamfunction fields based on the current meter data of the Texas-Louisiana Shelf Circulation and Transport Processes Study. Adopted here for the objective mapping is a method employing a two-dimensional truncated Fourier representation of the streamfunction over a domain, with the amplitudes determined by least square fit of the observation. The fitting was done with depth-averaged flow rather than depth-integrated flow to reduce the root-mean-square error. The fitting process filters out 11% of the kinetic energy in the monthly mean transport fields. The shelf-wide pattern of streamfunction fields is similar to that of near-surface velocity fields over the region. The nearshore transport, about 0.1 to 0.3 Sv (1 Sv=10^6 m^3/sec), is well correlated with the seasonal signal of along-shelf wind stress. The spring transport is weak compared to other seasons in the inner shelf region. The transport along the shelf break is large and variable. In the southwestern shelf break, transport amounts up to 4.7 Sv, which is associated with the activities of the encroaching of energetic anticyclonic eddies originated in Loop Current of the eastern Gulf of Mexico. The first empirical orthogonal function (EOF) of streamfunction variability contains 67.3% of the variance and shows a simple, shelf-wide, along-shelf pattern of transport. The amplitude evolution of the first EOF is highly correlated (correlation coefficient: 0.88) with the evolution of the along-shelf wind stress. This provides strong evidence that the large portion of seasonal variation of the shelf transport is wind-forced. The second EOF contains 23.7% of the variance and shows eddy activities at the southwestern shelf break. The correlation coefficient between the amplitudes of the second EOF and wind stress is 0.42. We assume that this mode is coupled a periodic inner shelf process with a non-periodic eddy process on the shelf break. The third EOF (accounting for 7.2% of the variance) shows several cell structures near the shelf break associated with the variability of the Loop Current Eddies. The amplitude time series of the third EOF show little correlation with the along-shelf wind.

Key words: volume transport, shelf circulation, ocean current, Texas-Louisiana shelf

Introduction

The volume transport of ocean is an important descriptive feature of the ocean circulation. Especially, the transport information over continental shelf is an essential element in understanding many human activities over the region. The Texas-Louisiana continental shelf, located at the northwestern part of the Gulf of Mexico, is important area in fishery, gas and oil industry. However, the current observations on the shelf have been quite limited and sparse before the Texas-Louisiana Shelf Circulation and Transport Study (LATEX). LATEX collected an extensive set of moored current meter data during the 32-month period from April 1992 through November 1994 (Jochens and Nowlin, 1994). The direct current measurements collected in LATEX now allow a unique opportunity for independent assessment of shelf volume transport. In a previous paper, Cho et al. (1998) presented near-surface velocity streamfunction fields based on the LATEX current data. The present paper is directed at understanding the shelf-wide transport pattern, its variability, and possible forcing mechanism with an objective description of the shelf-wide volume transport. The purpose of it is to provide the quantitative description of the volume transport on the Texas-Louisiana continental shelf.

The advantage using current meter data for transport calculation lies in simultaneous and almost continuous nature of the data over time, in contrast to hydrographic data. Also the transport estimated from hydrographic data does not include

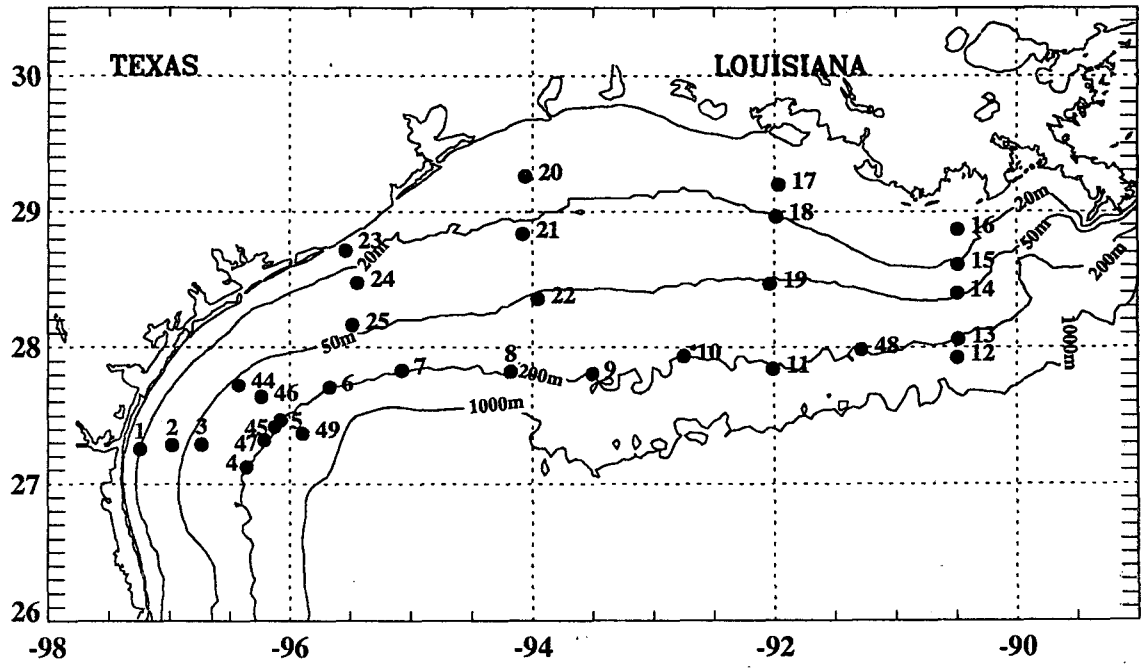

Fig. 1. Map of the Texas-Louisiana continental shelf showing the locations of current meter moorings by the Texas-Louisiana Shelf Circulation and Transport Processes Study (LATEX).

barotropic component of flow, which could bring a bias of true value. The disadvantage of LATEX current meter data lies in poor spatial (both horizontal and vertical) resolution. In order to overcome this, we try to produce the low-frequency and large-scale feature (having large coherent scale) of volume transport over the shelf. Our results are also compared with a numerical experiment by Oey (1995).

Next section describes the current meter data and its processing. The method for producing transport streamfunction is also presented in this section. The mean and variability of shelf-wide transport are addressed in the result section with the empirical orthogonal function (EOF) analysis of the streamfunction. We conclude the paper with a discussion and summary.

Data and Method

1. Data

The data used for the present study are the moored current meter measurements observed on the entire Texas-Louisiana continental shelf from April 1992 to November 1994 as a part of LATEX. The array consists of 75 current meters measuring current speed and direction, temperature, and conductivity on 31 moorings (Figure 1). The mooring positions and current meter depths are listed in Table 1. Five types of current meters (Endeco 174 SSM and DMT, Aanderaa RCM 4/5 and 7/8, and InterOcean S4) were deployed in the moorings. The mooring array was designed to identify a variety of physical processes on the Texas-Louisiana shelf and consisted of several sub-arrays (Nowlin *et al.*, 1991). In water shallower than 50 m, the mooring has two meters at depths near 10 ~12 m and near bottom. In water depth equal to or deeper than 50 m, meters were placed near 10~12 m, at mid-depth, and near the bottom, except for moorings 12, 44, and 45, which had only two meters (Jochens and Nowlin, 1994).

The current meters recorded the speed and direction of flow at 5-min to 2-hr interval (mostly at 30-min). Raw data were first filtered by a 3-hour low-pass Lanczos filter to reduce sampling noise, and then the filtered time series data were resampled at a 1-hr interval. The hourly data set was then filtered by a 40-hr low-pass Lanczos filter (Harris, 1978) having a width of 193 points of symmetric weight with a half-amplitude point of 40 hours to eliminate the tidal and inertial motions that are energetic on the shelf (Chen *et al.*, 1995). The 40-hr low-pass data were subsampled at 6-hr intervals. These data were used in this study.

2. Method

We employed a streamfunction representation

Table 1. The mooring number, water depth, position, and vertical depths of instruments of each LATEX A current meter mooring.

Mooring Number	Water Depth	Latitude (°N)	Longitude (°W)	Top CM Depth	Middle CM Depth	Bottom CM Depth
1	20	27.256	97.246	12 m		16 m
2	37	27.284	96.980	12 m		33 m
3	65	27.290	96.736	13 m	32 m	57 m
4	200	27.126	96.358	14 m	100 m	190 m
5	200	27.468	96.073	13 m	100 m	190 m
6	201	27.708	95.664	14 m	101 m	191 m
7	200	27.834	95.069	13 m	100 m	190 m
8	200	27.825	94.179	13 m	100 m	190 m
9	200	27.808	93.503	14 m	101 m	191 m
10	201	27.936	92.745	13 m	101 m	191 m
11	200	27.842	92.009	14 m	99 m	189 m
12	504	27.924	90.495	18 m	105 m	495 m
13	200	28.058	90.486	14 m	100 m	190 m
14	47	28.395	90.493	10 m	26 m	40 m
15	27	28.608	90.492	10 m		25 m
16	18	28.867	90.491	10 m		17 m
17	8	29.196	91.965	3 m		6 m
18	22	28.963	91.983	11 m		18 m
19	53	28.465	92.035	3 m	21 m	46 m
20	14	29.261	94.064	3 m		12 m
21	24	28.837	94.080	14 m		22 m
22	55	28.356	93.956	3 m	21 m	48 m
23	15	28.713	95.536	9 m		13 m
24	28	28.474	95.437	10 m		22 m
25	37	28.162	95.476	11 m	20 m	30 m
44	57	27.726	96.424	12 m		52 m
45	198	27.418	96.126	10 m	82 m	
46	91	27.638	96.234	10 m	50 m	84 m
47	204	27.322	96.213	19 m	104 m	194 m
48	201	27.983	91.283	15 m	101 m	191 m
49	502	27.369	95.894	14 m	102 m	493 m

for the objective mapping of the volume transport on the shelf. Our focus lies in the transport by low-frequency (quasigeostrophic) motion because the transport by high frequency motion is mainly periodic (Gill, 1982). In the coastal ocean, the low-frequency motion directs parallel to the isobath (along-shelf) due to the coastal boundary through the coastal Ekman pumping mechanism (Csanady, 1982). The momentum balance of the flow in the cross-shelf direction (perpendicular to isobath) is in geostrophic. In the along-shelf direction, the wind stress is balanced with the bottom friction. Thus the flow has a strong non-divergent component which can be represented by streamfunction field such as the studies of Gill and Schumann (1974) and Mitchum and Clarke (1986) in which both models deal with wind-driven flow. In addition to the extraction of the quasi-geostrophic component from the observation, the streamfunction analysis filters out the noise and divergent boundary Ekman flow. Another important objective employing stream-function on the shelf is that the field can be compared with the traditional geopotential anomaly study (Cochrane and Kelly, 1986).

For the generation of streamfunction, transport components per unit width (T_x, T_y) on each mooring are estimated from the following weighted sum of measured velocity:

$$T_x = \sum_{k=1}^{K} h_k U_k \text{ and } T_y = \sum_{k=1}^{K} h_k V_k \quad (1)$$

where K is the number of instruments on each moorings (3 at most) and h_k is the range of depth covered by the kth current meter. Of course h_k must be such that their sum equals the total depth at the mooring.

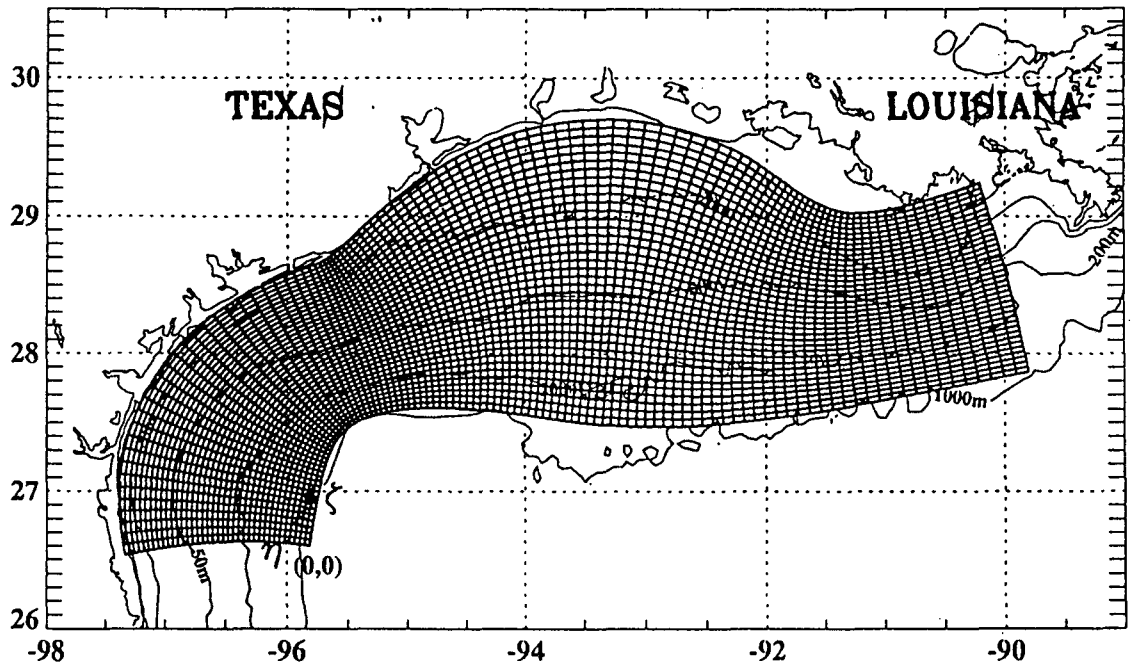

Fig. 2. The orthogonal, boundary-fitted curvilinear grid used for the transport streamfunction fields over the Texas-Louisiana shelf.

Of the two methods for estimating streamfunction fields employed by Cho (1996), the method which employes a representation in terms of domain structure functions is adopted in this study for the reasons: this method avoids the uncertain amount of the vorticity field required by the Poisson equation from the discrete array of mooring data, and provides an estimate of the streamfunction field that minimizes the variance of transport not represented by the selected structure functions employed in the fitting procedure.

Implementation of the method is done by employing a boundary-fitted orthogonal coordinate system (ξ, η) in which coastal boundary condition is easily specified and the offshore (seaward) boundary can be aligned along an isobath. In generation of the boundary-fitted grid of the present study the methodology developed by Mellor (1993) is used. Figure 2 shows the full grid generated by this method. The inshore and offshore boundaries are fitted to smoothed versions of the coast and the 1000-m isobath. In this coordinate system the water depth h is strongly dependent on the cross-shelf coordinate η and only weakly dependent on the along-shelf coordinate ξ. This makes it possible to separate the cross-shelf structure functions, constrained by zero at shore, from the along-shelf Fourier basis functions of arbitrary phase relative to the lateral open boundaries.

In the adopted method, the transport streamfunction ψ is represented in terms of a series of trigonometric basis functions in the boundary fitted coordinates as follows:

$$\psi(\xi,\eta)=\sum_n\sum_m(A_{n,m}\cos m\alpha\xi+B_{n,m}\sin m\alpha\xi)\sin n\beta\eta \quad (2)$$

where $\alpha=\pi/L_\xi$, $\beta=\pi/2L_\eta$; ξ and η represent the along- and cross-shelf axes; L_ξ and L_η represent the along- and cross-shelf ranges of the domain; and $A_{n,m}$ and $B_{n,m}$ are coefficients to be determined. The summations are limited to n and m in the range from 1 to N and M respectively. The $N\times M$ matrices of coefficients $A_{n,m}$ and $B_{n,m}$ are obtained by minimizing the following error measure:

$$\sigma^2=\frac{1}{j_{\max}}\sum_j[(\tilde{u}-\overline{u_j})^2+(\tilde{v}-\overline{v_j})^2], \quad (3)$$

where

$$\tilde{u}=-\frac{1}{h}\frac{\partial\psi}{\partial\eta}=-\sum_n\sum_m\frac{1}{h}(A_{n,m}\cos m\alpha\xi+B_{n,m}\sin m\alpha\xi)\,n\beta\cos n\beta\eta \quad (4)$$

$$\tilde{v}=\frac{1}{h}\frac{\partial\psi}{\partial\xi}=\sum_n\sum_m\frac{1}{h}(-A_{n,m}\sin m\alpha\xi+B_{n,m}\cos m\alpha\xi)\,m\alpha\sin n\beta\eta \quad (5)$$

and h is water depth, and $\overline{u_j}$, $\overline{v_j}$ are ξ and η

components of observed depth-averaged flows. For the coefficients of (2), the least square fitting is applied to the depth-averaged flow rather than depth-integrated field in order to reduce the root-mean-square (rms) error (3) of the fitting. At the coastal boundary $\eta=0$, the streamfunction and cross-shelf flow are automatically zero in the equation (2).

The observed transport is transformed into the orthogonal boundary system and then the streamfunction amplitudes are obtained by minimizing the equation (3) for a selected total number of harmonics. A linear set of equation for the coefficients is solved using standard lower/upper triangular (LU) decomposition techniques (Press *et al.*, 1986). The rms error of the fitting is computed using equation (3), which assumes that the error variance is isotropic.

Results

1. Record-length means

In this section, we examine the shelf-wide pattern of transport streamfunction on the Texas-Louisiana shelf. The primary objective is to produce large-scale structure of transport pattern having large spatial coherency, in which we intend to overcome the poor spatial resolution of the LATEX data.

Transport streamfunction fields based on the depth-averaged flow averaged over fixed periods can be generated using different combinations of M harmonics in the along-shelf and N in the cross-shelf directions. Increasing the number of Fourier harmonics reduces the rms error of fitting, but results in noisy patterns of streamfunction (Cho, 1996). A reasonably smooth streamfunction pattern demands the use of lower harmonics at the expense of higher rms error. The number of degrees of freedom of observation field is at most 62 (counting both current components). In fact, in many cases of the monthly mean fields, the degrees of freedom are significantly decreased by lack of current meter data, thus demanding the use of fewer harmonics. Although the number of harmonics that produces a reasonably smooth streamfunction pattern is not same for different monthly mean transport fields, for simplicity we adopted the fixed combination $M=3$ and $N=2$ through the remainder of this study. Cho (1996) has shown that this combination gives results qualitatively consistent with the Poisson method of estimation. It will be noted that the total number of degrees of freedom in the fitted streamfunction patterns is $2MN$, giving twelve for the adopted M and N.

One of the dominant characteristics of the low-frequency circulation in the Texas-Louisiana shelf is the contrast between summer and nonsummer seasons (Cochrane and Kelly, 1985; Oey, 1995; Cho, 1996; Cho et al., 1998). Thus we first calculated the transport streamfunction fields based on the record-length nonsummer and summer means. The root mean square (rms) residual errors (3) are 2.64 cm/sec for the nonsummer and 3.56 cm/sec for summer. The rms errors can be compared with the depth-averaged speed of 6.17 cm/sec for nonsummer and 6.39 cm/sec for summer. The ratios of the two values are 0.41 for nonsummer and 0.58 for summer (0.17 and 0.34 in relative error variance). The rms error accounts for discrepancies in both speed and direction. The ratio of nonsummer is comparable to the those of other studies (Vastano and Reid, 1985; Barron, 1994; Cho, 1997). The summer rms error has somewhat higher value, which suggests that portion of kinetic energy is filtered out by the fitting process.

The transport streamfunction fields are calculated by the equation (2) on the grids of Figure 2 and then contoured in Figure 3 (nonsummer mean: upper panel, summer mean: lower panel). The contours of transport streamfunction are not uniform due to the large intervals within the shelf but vary as follows: 0.05, 0.1, 0.3, 0.5, 1, 3, 5 Sv (1 Sv$=10^6$ m^3/sec). The pattern can be compared to the dynamic height field (Cochrane and Kelly, 1985) and mean velocity streamfunction field (Cho et al,. 1998). During the nonsummer regime, downcoast transport is well established and transport in the range of 0.1 to 0.3 Sv over the inner shelf. During the summer, coastal flow is directed upcoast and transport amounts to about 0.1 Sv in the inner shelf. Transports are larger in deeper water. As first suggested by Cochrane and Kelly (1986), the summer and nonsummer circulation regimes on the inner shelf are well correlated with the along-shelf component of the wind stress. During the LATEX field measurement period (April 1992 through November 1994), a dense network of sites over the northwestern Gulf of Mexico existed from which wind velocity measurements were available. Hourly fields of 10-m level wind velocity component were derived by Wang (1996) using optimal statistical interpolation. From these, she

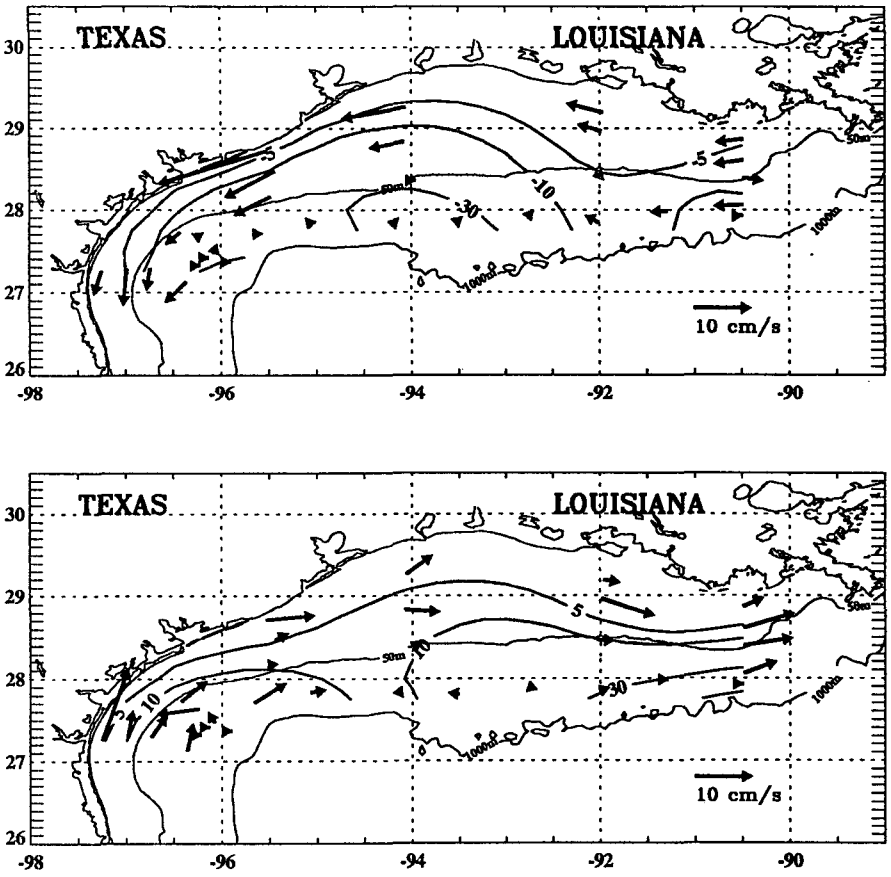

Fig. 3. Shelf-wide record-length mean transport streamfunction field for nonsummer (upper panel) and summer (lower panel). Arrows represent depth-averaged mean vectors. The unit of streamfunction is 10^{10} cm^3/sec (0.01 Sv).

constructed hourly along-shelf components of wind stress at six locations nearly equally spaced along the 20-m isobath between 90.5° W and 26.0° N. From this information, monthly averages of the along-shelf stress components were evaluated, and then an average of these six values was obtained for each of the first 13 months among the LATEX measurement period. The resulting sequence (Figure 4) characterizes the wind forcing on the inner shelf and shows downcoast forcing during the non-summer regimes and upcoast forcing during the summer regimes, which matches the direction of nearshore current shown for the mean nonsummer and summer transport patterns in Figure 3. We will find the detailed monthly sequence of along-shelf stress presented in Figure 4 very useful in discussing seasonal patterns of transport presented in the following section. Moreover, the forcing index given in Figure 4 will be related quantitatively to the amplitudes of the statistically dominant patterns of transport.

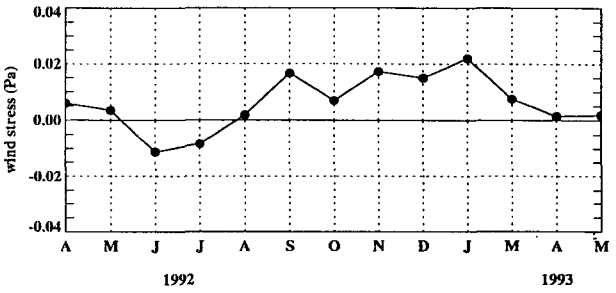

Fig. 4. Monthly mean along-shelf wind stress in the Texas-Louisiana inner shelf (20 m) from April 1992 to May 1993. The positive value is downcoast.

2. Seasonal patterns

Seasonal variation of the shelf-wide patterns of volume transport on the Texas-Louisiana shelf is described in this section. Considered are transport streamfunctions for the first 13 months from April 1992 to May 1993 (minus February 1993, which had insufficient data) due to the lack of data in other

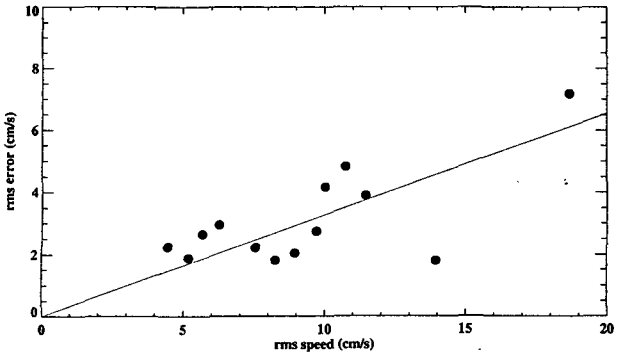

Fig. 5. Root-mean-square (rms) error of fit of monthly mean depth-averaged current data by transport streamfunction versus the rms depth-averaged speed for 13 months of LATEX data. A linear regression, constrained to go through the origin, is shown.

months. The rms errors of fit and corresponding rms speed are shown in Figure 5. As might be expected, all of the rms speeds associated with the monthly average fields of current data are greater than the rms error associated with the spatial pattern of the monthly average current data. The fitted linear regression (constrained to pass through the origin) has a slope of 0.33, indicating that on average the error variance is about 11 percent of the variance of the current speed. In other words, the monthly patterns of transport have filtered out about 11 percent of the kinetic energy in the method of fitting with resolution consistent with that of the observational mooring array. The small residual values indicate that the transport fields are reasonably well represented by the streamfunction defined as equation (2).

Figure 6~9 show 8 monthly mean maps of transport streamfunction. They are arranged into two-month maps for each season so as to compare different seasons. Each figure shows the monthly mean depth-averaged current as well as the fitted streamline contours. Spring (April and May, 1992) patterns of transport streamfunction field (Figure 6) show weak downcoast transports over the inner

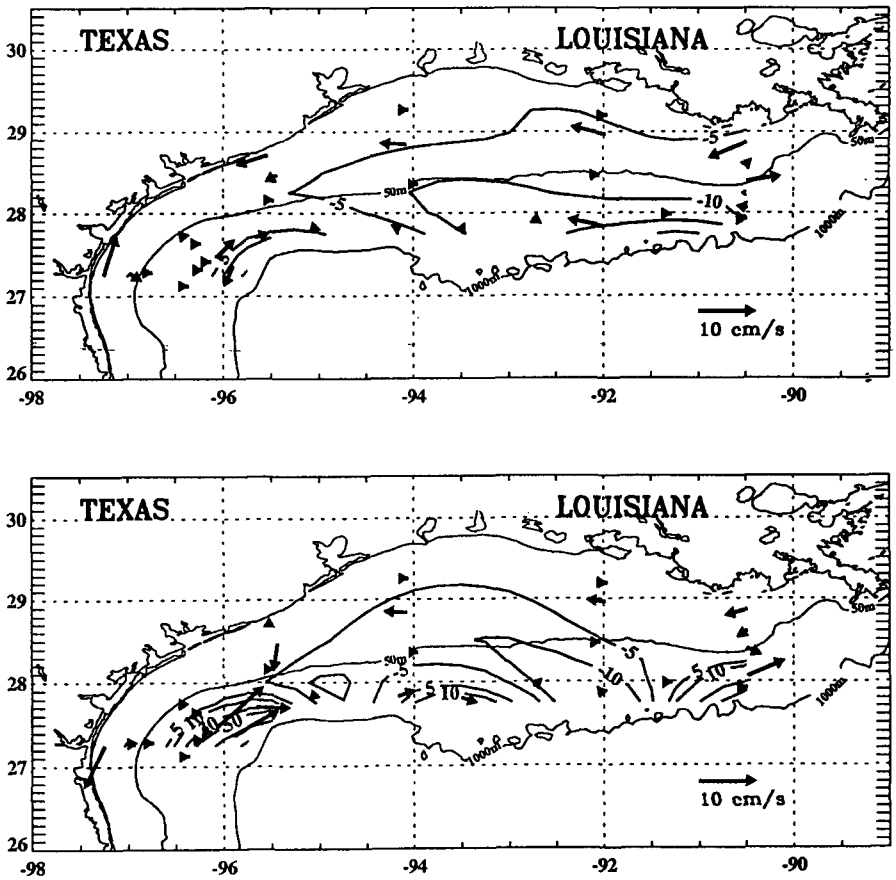

Fig. 6. Shelf-wide monthly mean transport streamfunction field for spring (upper panel: April 1992, lower panel: May 1992). Arrows represent monthly depth-averaged mean vectors. The unit of streamfunction is 10^{10} cm^3/sec (0.01 Sv).

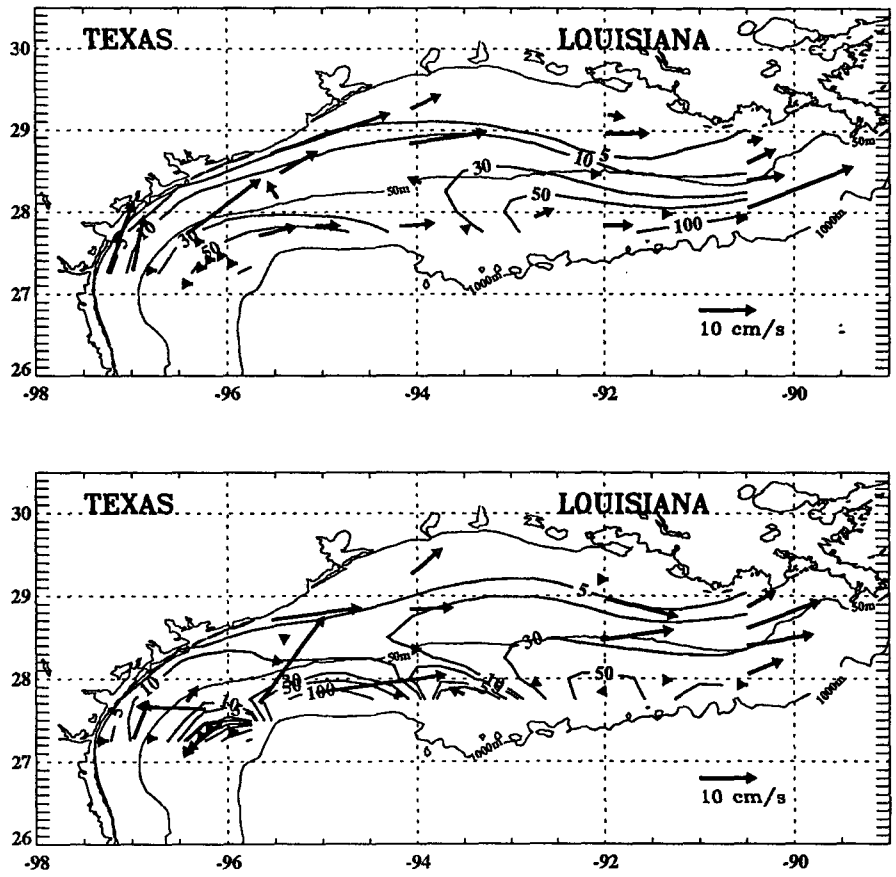

Fig. 7. Shelf-wide monthly mean transport streamfunction field for summer (upper panel: June 1992, lower panel: July 1992). Arrows represent monthly depth-averaged mean vectors. The unit of streamfunction is 10^{10} cm^3/sec (0.01 Sv).

and middle shelf. Transport from inner measurements to mid-shelf (50 m) is about 0.05 to 0.1 Sv. Along the shelf break, the upcoast transport is shown, thus forming a cyclonic cell over the shelf. But the upcoast transport in the shelf break is not continuous along the shelf. On the southwestern shelf edge, a relatively large upcoast transport (2.3 Sv) is seen in May of 1992 (lower panel of Figure 6) and probably related to a Loop Current Eddy (LCE). The relatively weak transport in this season would be related to the weak along-shelf wind stress for the spring (Figure 4).

The summer (June and July, 1992) patterns of streamfunction field (Figure 7) show upcoast transport over both inner and outer shelf consistent with the wind forcing index (Figure 4). The transition from the nonsummer to summer pattern of along-shelf wind stress and of resulting upcoast along-shelf transport had been completed during these months. The amount of transport increases with depth and is 0.2 to 0.3 Sv from inner shelf to mid-shelf. Inner shelf transports are larger than those of spring due to the larger wind forcing during this season (Figure 4). In June onshelf transports across the 50-m isobath are seen over the central shelf. Several small cell structures are shown along the shelf break, especially in the pattern of July 1992 (lower panel of Figure 7).

The return to a downcoast circulation over the inner shelf usually occurs near the end of August because of the transition to downcoast along-shelf wind component (Cochrane and Kelly, 1985). In September 1992, the pattern (upper panel of Figure 8) shows downcoast transport over the entire shelf. Along the shelf break, the upcoast transport is not shown in this month. The downcoast transport amounts to 0.3 - 0.5 Sv between inshore observations and mid-shelf. This relatively strong inner shelf transport is compared to the those of spring and summer of 1992 and also the wind forcing index (Figure 4). This result also supports Oey's numerical experiment (1995), which showed

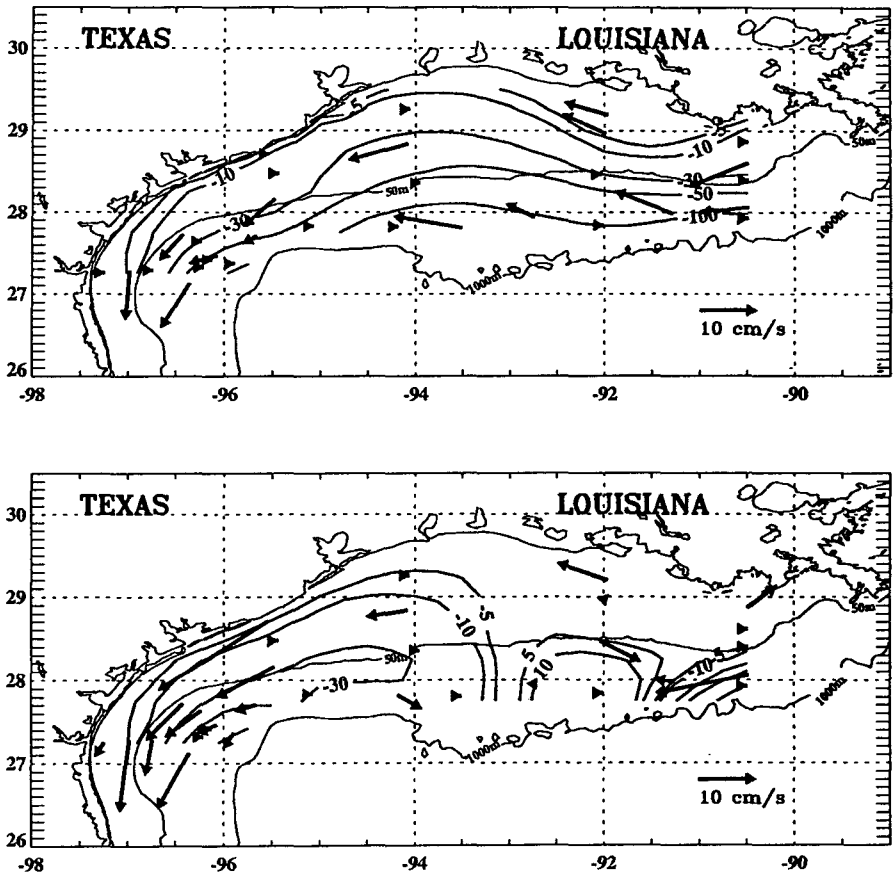

Fig. 8. Shelf-wide monthly mean transport streamfunction field for fall (upper panel: September 1992, lower panel: October 1992). Arrows represent monthly depth-averaged mean vectors. The unit of streamfunction is 10^{10} cm^3/sec (0.01 Sv).

maximum transport during fall. In October 1992 (lower panel of Figure 8), pattern is shifted downcoast direction with onshore transport over the central shelf. The amount of the transport for the month is somewhat reduced compared to that of September in the central and eastern inner shelf region. The transport along the shelf break shows large variability. There was an anticyclonic cell structure over the eastern outer shelf.

In the winter (December 1992 and January 1993), the well established downcoast transport over the inner shelf had been continued (Figure 9). The pattern of the inner shelf transport is also consistent with the forcing index (Figure 4). Overall pattern of winter is similar with fall in the inner shelf. The transport over inner shelf is about 0.3 Sv. The transport along the shelf break is variable and very large (4.7 Sv in December and 3.7 Sv in January) over the southwestern area of shelf break. This large transport over the region is related to the Eddy Vasquez (Jochens et al, 1997). Figure 10 shows the monthly mean near-surface flow field from November 1992 to January 1993, showing the evolution of the Eddy Vasquez (Jochens et al, 1997) in the southwestern area of the shelf break.

In summary, the monthly transport streamfunctions for the shelf-wide pattern shows a distinct contrast between nonsummer (September -May) and summer (June-August) whose general features support the Cochrane and Kelly (1985) schema, although there are some cases where the sparseness of data for given month produces doubtful patterns. Along the shelf break, the transport is variable and relatively large especially over the southwestern area which is called the tomb of the LCEs (Oey, 1995).

3. EOFs

The time series of monthly mean transport streamfunction over the shelf can be described in terms of EOFs. Mathematically, EOFs are the eigenvectors from a data covariance matrix, and are a very efficient tool for quantifying principal patterns in geophysics data (Kundu et al., 1975; North et al., 1982; Preisendorfer and Mobley, 1988).

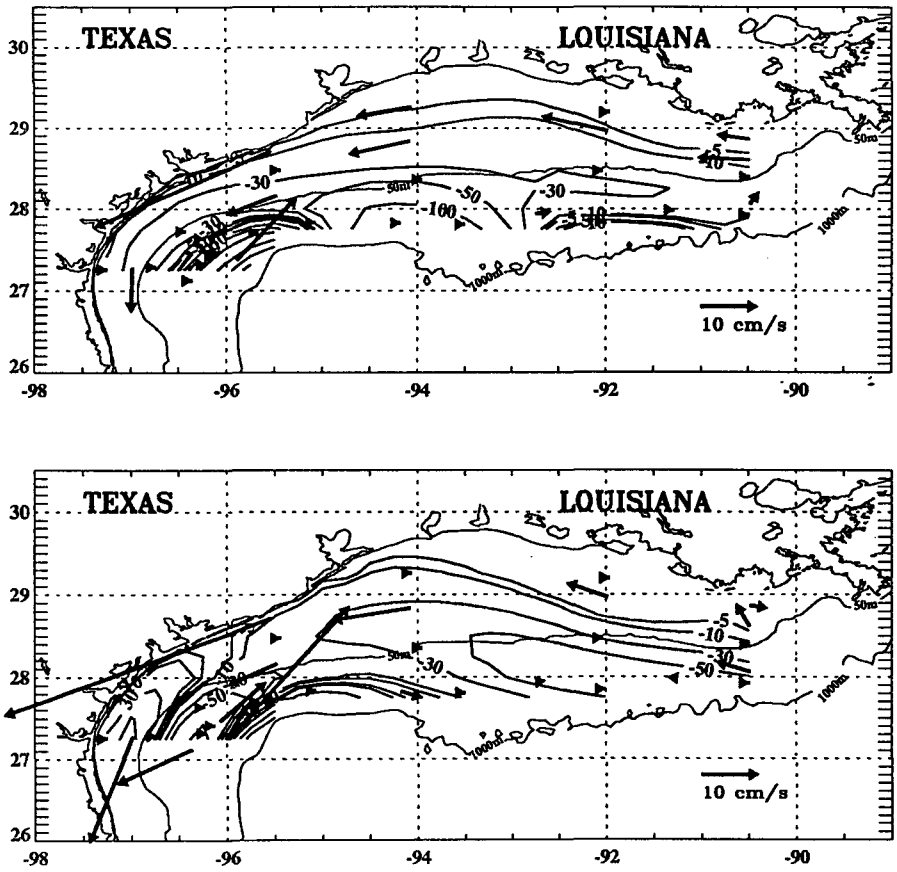

Fig. 9. Shelf-wide monthly mean transport streamfunction field for winter (upper panel: December 1992, lower panel: January 1993). Arrows represent monthly depth-averaged mean vectors. The unit of streamfunction is 10^{10} cm^3/sec (0.01 Sv).

In the present application the matrix is that formed from the product of monthly transport streamfunction anomaly at grid point j on the shelf with that at grid point k. The streamfunction anomaly at point j is defined as the value for given month m minus the value at point j corresponding to the record length mean field. Thus the covariance $R(j, k)$ of the anomalies so defined at point j and k is a measure of the covariability at these points after removal of the mean field. The covariance estimate $R(j,k)$ is obtained by averaging anomaly products at j and k over all months m (13 in the present case). The eigenvalues of the symmetric matrix $R(j, k)$ represent the variance associated with a given eigenvector. The dominant pattern (first EOF) is defined by that eigenvector associated with the largest eigenvalue, the second EOF has the next largest eigenvalue, and so on.

The total number of non-zero EOF eigenvalues is 12, corresponding to the degrees of freedom in the harmonic representation of the streamfunction fields. The sample eigenvalues for all 12 modes are given in Table 2 (note the mode 12 is not zero but 0.0024%). Of these twelve EOF modes only first three EOF patterns are shown here, since the North et al (1982) test for statistical validity indicates that all modes beyond the third are considered noise, in the sense that their associated EOF patterns are not unique for the given data sample. The first three EOFs are shown in Figure 11 and their amplitude time series in Figure 12. These three EOFs comprise about 96% of the total mean square variability.

The first EOF contains 67.3% of the variance and has a very simple shelf-wide structure of along-shelf transport over the entire shelf. The amplitude time series of the first EOF are generally characterized by positive values (downcoast transport- directing to the Mexico) during the nonsummer season and negative values (upcoast transport-directing to Florida) during the summer season. However, negative values in the first mode amplitude are also seen in May 1992 and March 1993. The amplitude

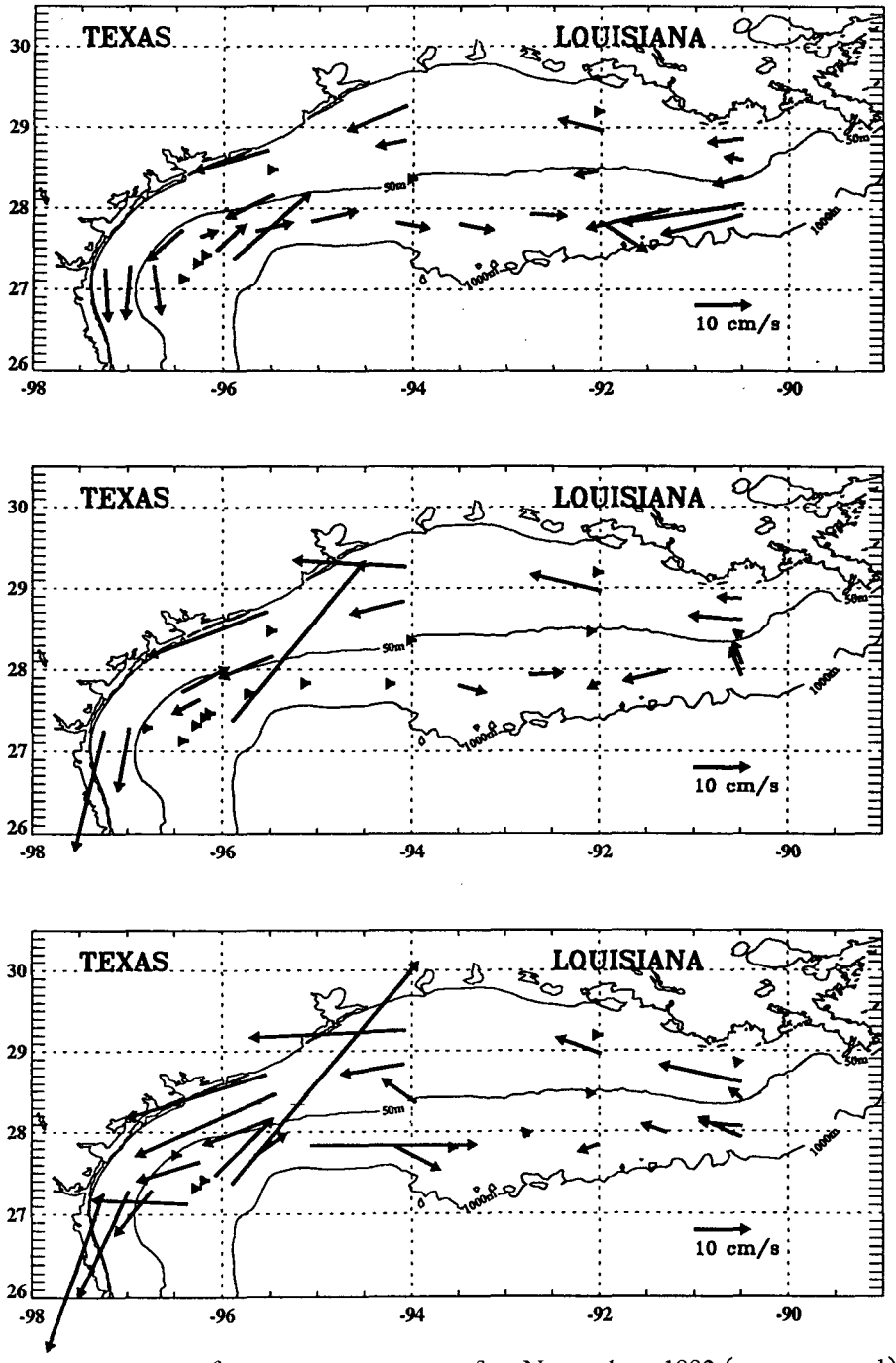

Fig. 10. Monthly mean near-surface current vectors for November 1992 (upper panel), December 1992 (middle panel), and January 1993 (lower panel).

time series are very similar to the evolution of the along-shelf wind stress during the period (Figure 4). The correlation coefficient of the two sequences is 0.88, providing strong evidence that the wind stress over the shelf is the dominant forcing for the first EOF pattern (67% of variance) of transport on the Texas-Louisiana shelf.

The second EOF accounts for 22% of the variance and the pattern is similar to the first EOF in the inner shelf region. This mode shows strong eddy influence at the southwestern shelf break. The correlation coefficient between wind stress and the EOF amplitude time series is 0.42. It is assumed that this mode is coupled with a periodic inner shelf process and a non-periodic shelf break LCE process.

Table 2. Eigenvalues in percent for the EOF modes.

Mode	Eigenvalues
1	67.26
2	21.60
3	7.02
4	1.95
5	1.03
6	0.58
7	0.25
8	0.17
9	0.09
10	0.03
11	0.02
12	0.00
sum	100

The third EOF occupies 7.2% of the variance and has several cell structures along the outer shelf, thus providing on- and offshore transports over the shelf. The amplitude of this mode do not have a seasonal pattern, and there is no correlation (correlation coefficient: 0.11) between the monthly mean wind stress of Figure 4 and the amplitude time series of the third EOF given in Figure 12. The third EOF pattern seems to be related with the shelf break processes which show large variability in the monthly transport streamfunction maps.

Discussion and Summary

As stated in the introduction, the ultimate intent of the present study is to provide the quantitative description of the volume transport on the Texas-Louisiana continental shelf. The current meter data used here have vertical resolutions with only two or three current meters on each mooring and thus the results of the present study can be regarded as first estimate which will surely be revised in the future. However, justification to overcome the limitation of the LATEX current meter data is multi-fold. Firstly, the vertical current structure on the shelf is to be known as generally monotonic by former studies (Smith, 1979; Kelly et al., 1985; Chen, 1995). Secondly, we concentrated on the volume transport composed of low-frequency motion, which has a large coherent spatial scale and non-divergent nature. For the purpose, we first filtered out the high-frequency motions such as inertial and tidal motions. We also adopted a methodology of streamfunction representation, which extracts the non-divergent part of flow. In the streamfunction generation, we used the limited number of harmonics in order to produce shelf-wide simple structure. Finally, Clarke and Brink (1985) suggested that the shelf response to wind is primarily barotropic when the bottom slope of the shelf (α), Coriolis parameter (f), and shelf-averaged buoyancy frequency (N) satisfy the condition $N\alpha/f \ll 1$. The value of this parameter is less than 10^{-2} on the Texas-Louisiana shelf according to Barron (1994).

To deduce the shelf-wide volume transport from discretely sampled current data, we chose a representation method of volume transport streamfunction, thus constraining the estimated transport to be horizontally non-divergent field similar to geostrophic flow on a f-plane. Estimates of streamfunction fields can be produced in several way. Adopted here is a method (Vastano and Reid, 1985; Cho, 1997) employing a two-dimension truncated Fourier representation of the streamfunction over a domain, with the amplitudes determined by least square fit of the velocity data. This method avoids the uncertain estimation of the vorticity field required by the Poisson method (Hubertz et al, 1972; Cho, 1997) from the discrete array of mooring data and provides an estimate of the streamfunction field that minimizes the variance of transport not presented by the selected structure functions employed in the fitting procedures. The fitting was done with depth-averaged flow rather than depth-integrated one to reduce the rms error. We used 12 number of modes in the structure function (3 in the along-shelf direction and 2 in the cross-shelf direction). So the degree of freedom is 12 in the fitted streamfunction pattern. The nondivergent part of transport in the fitting process recovers 83% of the kinetic energy for the record-length nonsummer mean field and 66% for the summer mean field. In the monthly mean field, the objective mapping filters out about 11 % of the kinetic energy (Figure 5).

In general, monthly mean transport increases with water depth. This was expected since the depth-averaged current speed is of about the same order of magnitude over the shelf, while water depth varies by an order of magnitude. The nearshore transport amounts to about 0.1 to 0.3 Sv from nearshore observation to the mid-shelf (50 m). There was a large transport (up to 4.7 Sv) associated with a offshore LCE near the shelf break in the southwest of the study area. This results generally support the numerical experiment by

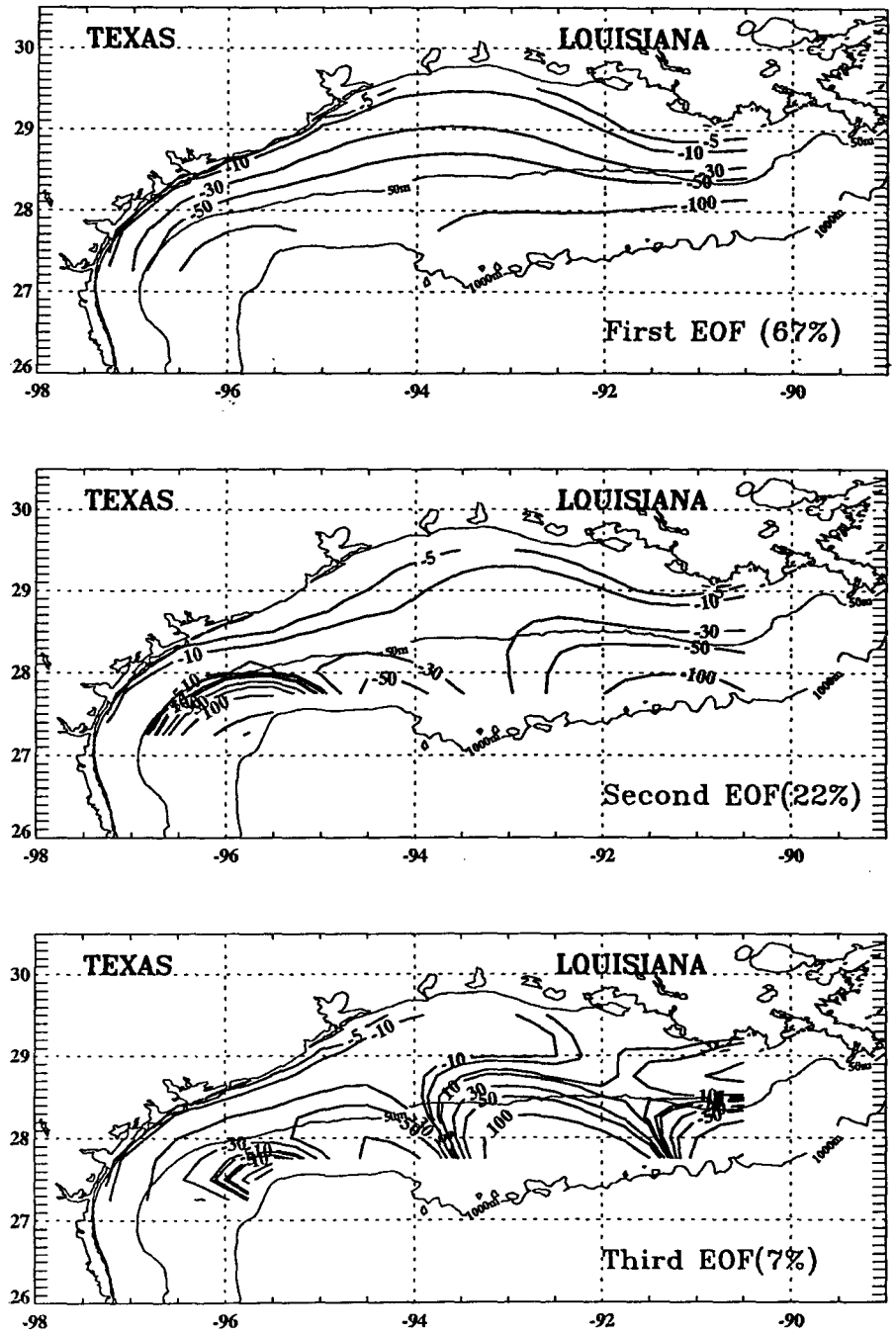

Fig. 11. Contours of the first three EOFs calculated from the 13 monthly mean transport streamfunction fields. The percent of variance accounted for by each mode is indicated.

Oey (1995). The shelf-wide pattern of transport streamfunction has a very similar structure to that of the near-surface velocity streamfunction field (Cho et al, 1998), in that transport is directed downcoast during the nonsummer and upcoast during the summer. In the inner shelf, the transport is well correlated with the wind stress forcing index (Figure 4). This result coincides the former studies (Cochrane and Kelly, 1986; Oey, 1995; Cho et al., 1998) which recognized the importance of the seasonal signal in the along-shelf component of wind stress and its correlation with the seasonal signal of the near coastal along-shelf current. This reveals that the large portion of the transport in the inner shelf comes from the along-shelf jet formed through a coastal Ekman pumping mechanism (Csanady, 1982). Along the shelf break, the transport does not have a continuos pattern which was drawn in the

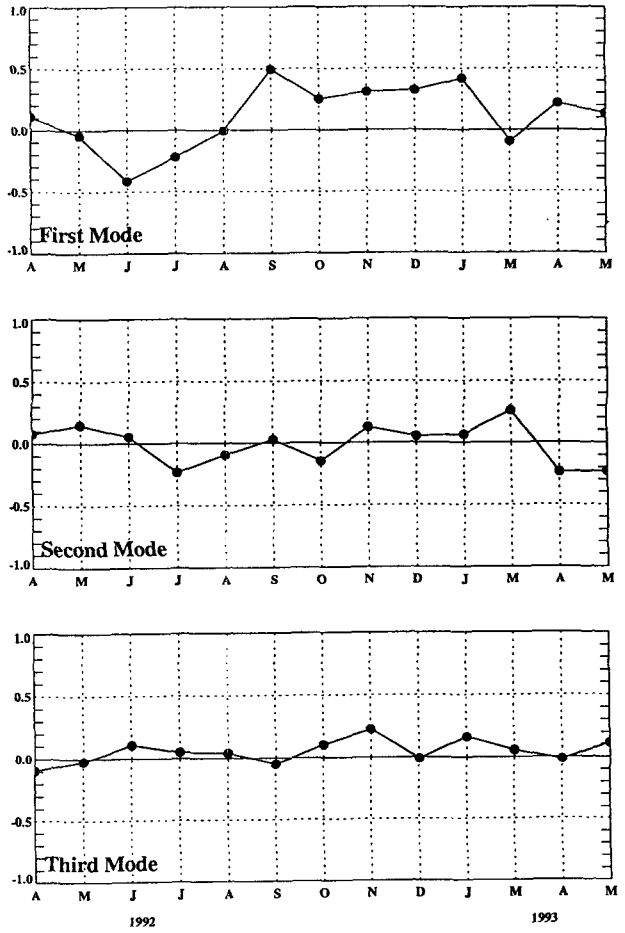

Fig. 12. The amplitude (10^{10} cm^3/sec) time series over 13 months for the first (upper panel), second (middle panel) and third (lower panel) EOFs.

dynamic height field (Cochrane and Kelly, 1986) and numerical experiment (Oey, 1995) but shows several cell structures. The transport along the shelf break, especially in the southwestern area of shelf, is influenced by the activities of the encroaching of energetic anticyclonic eddies along the seaward shelf edge (Figure 10). These eddies have their origin in the Loop Current of the eastern Gulf of Mexico, from which they separate and drift into western Gulf and seem to be attracted particularly to the bight region off the western Texas shelf (Elliott, 1982). LCEs experience a collision and stalling processes over the southwestern area of the shelf and then direct upcoast along the shelf break, decaying fast after the turning. The processes of LCE influence the flow and transport over the shelf, especially over the shelf break.

The dominant first EOF pattern of variability shows a simple shelf-wide pattern of unidirectional along-shelf transport. This EOF mode accounts for 67% of the monthly variance. The amplitude of the first EOF mode is highly correlated with the seasonal variation of wind, while the second mode is moderate and third mode is little, implying that wind is the primary forcing for seasonal variation of shelf-wide, low-frequency transport over the Texas-Louisiana shelf. Thus the wind-forcing as defined in Figure 4 serves as a very robust index of low-frequency, wind-induced, shelf-wide upcoast or downcoast transport on the Texas-Louisiana shelf. In the generation of streamfunction, we used structure functions only having 12 degrees of freedom due to the poor spatial resolutions of data, resulting in suspecting pattern of streamfunction in certain months. The monthly mean streamfunction pattern can be reconstructed using the fitted EOF representation. We expect that the well determined pattern will not change much, but the suspect pattern will become more realistic via fitted EOFs.

In a summary, seasonal volume transport over the Texas-Louisiana continental shelf is investigated in terms of objectively fitted transport streamfunction fields based on the LATEX current meter data. The objective fitting filters out 11% of the kinetic energy in the monthly mean field, indicating that the transport fields are represented reasonably well by the streamfunctions. The shelf-wide pattern of transport streamfunction field is similar to near-surface velocity fields over the region. The nearshore transport, about 0.1 to 0.3 Sv, is well correlated with the seasonal signal of along-shelf wind stress. The transport along the shelf break, especially in the southeastern area of shelf, is associated with the activities of LCEs and amounts up to 4.7 Sv. The minimum transport occurred in spring and maximum in fall and winter. The first EOF which contains 67.3% of the variance shows a simple, shelf-wide, along-shelf pattern of transport. The high correlation between amplitude evolutions of the first EOF and the along-shelf wind stress provides strong evidence that the large portion of seasonal variation of the shelf transport is wind-forced. The second and third EOFs show the influence of LCEs.

Acknowledgement

I would like to thank all LATEX scientists and technicians who collected and quality controlled the current meter data used in this study. This study

was funded by the Mineral Management Service under OCS contract number 14-35-0001-30509. Additional funding has been provided by Texas A & M University, the Texas Engineering Experiment Station, and the Texas Institute of Oceanography. In the publication stage, I was supported by the Research Center of Ocean Industrial Development (RCOID), Pukyong National University.

References

Barron, C. N. Jr. 1994. Short interval prediction of surface motion on the Texas continental shelf. Ph. D. Dissertation, Texas A & M University, College Station, Texas, 133 pp.

Chen, H. W. 1995. Variability and structure of currents over the Texas-Louisiana shelf- A view from a shipboard acoustic Doppler current profiler. Ph. D. Dissertation, Texas A & M University, College Station, Texas, 103 pp.

Chen, C., R. O. Reid and W. D. Nowlin Jr. 1995. Near-inertial oscillations over the Texas-Louisiana shelf. J. Geophys. Res., 101, 3509~3524.

Cho, K. 1996. Three dimensional structure and variability of low-frequency currents Texas-Louisiana shelf based on moored current meter data. Ph.D. Dissertation, Texas A & M University, College Station, 121 pp.

Cho, K. 1997. Objective estimation of velocity streamfunction with discretely sampled data I: with application of Helmholtz theorem. J. Kor. Environ. Sci. Soc., 6 (4), 323~333.

Cho, K. 1997. Objective estimation of velocity streamfunction field with discretely sampled oceanic data II: with application of least-square regression analysis, J. Kor. Environ. Sci. Soc., 6 (5), 541~550.

Cho, K., R. O. Reid and W. D. Nowlin Jr. 1998. Objectively mapped streamfunction fields on the Texas-Louisiana shelf based on 32 months of moored current meter data. J. Geophys Res., 103 (C5), 10377~10390.

Clarke, A. J., and K. H. Brink. 1985. The response of stratified, frictional flow of shelf and slope waters to fluctuating large-scale, low-frequency forcing. J. Phys. Oceanogr., 15, 439~453.

Cochrane, J. D. and F. J. Kelly. 1986. Low-frequency circulation on the Texas-Louisiana continental shelf. J. Geophys Res., 91, 10645~10659.

Csanady, G. T. 1982. Circulation in the coastal ocean. D. Reidel, Holland, 279 pp.

Gill, A. E. 1982. Atmospheric-Ocean Dynamics, Academic Press, 662 pp.

Gill, A. E. and E. H. Schumann. 1974. The generation of long shelf waves by the wind. J. Phys. Oceanogr., 9, 975~991.

Elliott, B. A. 1982. Anticyclonic rings in the Gulf of Mexico. J. Phys. Oceanogr., 12, 1292~1309.

Harris, F. J. 1978. On the use of windows for harmonic analysis with the discrete Fourier transform. Proc. IEEE, 66, 51~83.

Hubertz, J. M., A. W. Garcia and R. O. Reid. 1972. Objective analysis of ocean surface current. Contributions on the Physical Oceanography of the Gulf of Mexico, Gulf Publishing Company, 139~148 pp.

Jochens, A. E., R. R. Leben and G. S. Fargion. 1998. Observation of loop current eddy Vasquez in the northeast Gulf of Mexico. J. Geophys. Res., in press.

Jochens, A. E. and W. D. Nowlin, Jr. 1994. Texas-Louisiana shelf circulation and transport processes study: Year, Annual Report, Mineral Management Service, 183 pp.

Kelly, F. J., J. E. Schmitz, R. E. Randall and J. D. Cochrane. 1985. Physical Oceanography, Chapter 1. Offshore Oceanographic and environmental monitoring services for the Strategic Petroleum Reserve. Report of the U.S. Dept. of Energy, Washington, DC. Report No. DOE/P010850-4.

Kundu, P. K., J. S. Allen, and R. L. Smith. 1975. Modal decomposition of the velocity field near the Oregon coast. J. Phys. Oceanogr., 5, 683~704.

Mellor, G. L. 1993. User's guide for a three-dimensional, primitive equation, numerical ocean model. Princeton University, 35 pp.

Mitchum, G. T. and A. J. Clarke. 1986. Evaluation of frictional, wind-forced long-wave theory on the west Florida Shelf. J. Phys. Oceanogr., 16, 1029~1037.

North, G. R., T. L. Cahalan and F. J. Moeng. 1982. Sampling errors in the estimation of empirical orthogonal functions. Mon. Wea. Rev., 110, 699~706.

Nowlin, W. D. Jr., A. E. Jochens, N. L. Guinasso Jr., D. A. Wisenburg, R. O. Reid, S. A. Hsu and R. C. Hamilton. 1991. Louisiana/Texas Physical Oceanography Program Task A, Technical Proposal. Texas A&M University, Reference No. 93-06-T, 181 pp.

Oey, L.-Y. 1995. Eddy- and wind-forced shelf circulation. J. Geophys Res., 100, 8621~8637.

Pedlosky, J. 1987. Geophysical Fluid Dynamics. Springer-Verlag, 624 pp.

Preisendorfer, R. W. and C. D. Mobley. 1988. Principal Component Analysis in Meteorology and Oceanography. Elsevier, 425 pp.

Press, W. H., B. P. Flannery, S. A. Teukolsky and W. T. Vettering. 1986. Numerical recipes. Cambridge University Press, 818 pp.

Smith, N. P. 1979. An investigation of vertical structure in shelf circulation. J Phys. Oceanogr., 9, 624~630.

Vastano, A. C. and R. O. Reid. 1985. Sea surface topography estimation with infrared satellite imaginary. J. Atmos. Oceanic Technol., 2, 393~400.

Wang, W. 1996. Analysis of wind field over the northwest Gulf of Mexico and the response of nearshore current to the wind forcing. Ph.D. Dissertation, Texas A & M University, College Station, 121 pp.